

Elastic pp and $\bar{p}p$ scattering in the models of unitarized pomeron

E. Martynov

Bogolyubov Institute for Theoretical Physics, 03143 Kiev, Ukraine.

E-mail: martynov@bitp.kiev.ua

February 8, 2020

Abstract

Elastic scattering amplitudes with pomeron singularity by construction meeting the main unitarity bounds valid at high energy are considered. Restrictions for a form of pomeron singularity are stressed. The models of double and triple (at $t = 0$) pomeron pole with additional terms important for low energies are compared with all existing experimental data on pp and $\bar{p}p$ total and differential cross sections at $\sqrt{s} \geq 5$ GeV and $|t| \leq 6$ GeV². Good agreement with data is obtained for both models, however the dipole pomeron model gives a slightly better description of the data. Predictions made for the LHC energy demonstrate a big enough difference of the models at $t \approx -0.4$ GeV². Such a difference, apparently allows to choose a more reasonable model after TOTEM measurements.

Keywords: Hadron elastic scattering

PACS: 13.85.-t, 13.85.Dz, 11.55.-m, 12.40.Na, 13.60.Hb

1 Introduction

The forthcoming experiments of TOTEM at the LHC will be in fact the first measurement of soft pomeron (more strictly, pomeron and odderon), because the secondary reggeon contributions would be so small at 14 TeV that they can be neglected. Therefore the precise measurement of pp differential cross section gives a chance to distinguish various models of pomeron. To do this one need to have and compare the predictions of the models. Such a comparison makes a sense only if the same data set is used when parameters of the models are determined.

There are three kinds of models for elastic hadron scattering amplitudes that reproduce rising cross sections with a reasonable precision.

- Models in which pomeron (as well as odderon) is a simple pole in a complex momentum plane located righter of unit, $\alpha_P(0) = 1 + \varepsilon \approx 1.1$ [1, 2]. To describe a dip-bump structure in differential cross section one should take into account cuts in one or another

form. Such a pomeron violates unitarity bound $\sigma_t(s) \leq C \ln^2 s$ at $s \rightarrow \infty$. However, the argument that unitarity corrections are important only at higher energies justifies the approach.

- Pomeron with $\alpha_P(0) > 1$ is an input in some scheme of unitarization (examples are eikonal or quasieikonal [3], U -matrix models [4]). When unitarization is performed all such models give $\sigma_t(s) \propto \ln^2 s$, whereas many other predictions depend on the type of model.
- The third way to construct amplitude is just from the beginning to take into account unitarity and analytical requirements as well as experimental information on the cross sections (e.g. growth of total cross sections). Such a model can be named as model of unitarized pomeron. The most successful examples are tripole pomeron ($\sigma_t(s) \propto \ln^2 s$) [5, 6, 7] and dipole pomeron ($\sigma_t(s) \propto \ln s$) [8, 9].

In this paper within the third approach we consider the models of tripole and dipole pomeron. These models are the best in a description of all data on the forward scattering data [10].

As it was shown in the papers [10, 11] total cross sections of meson and nucleon interactions are described with the best χ^2 in the dipole and tripole models in which forward scattering amplitudes were parametrized in explicit analytic form. This conclusion was confirmed when dispersion relations were applied for real part of amplitudes [12].

Small- $|t|$ ($0.1 \leq |t| \leq 0.5 \text{ GeV}^2$) elastic scattering ($pp, \bar{p}p, \pi^\pm p$ and $K^\pm p$) was analyzed in details in the [14]. The specific model was considered, in which hard pomeron contribution (with $\alpha_h(0) \approx 1.4$) is added to a soft one. It was motivated by observation made in [13] that such an additional pomeron allows strongly to improve a not enough good description of the meson and nucleon data on parameter $\rho = \Re A(s, 0) / \Im A(s, 0)$ in the model of simple pole pomeron with $\alpha_h(0) \approx 1.1$. Extension of the model to higher $|t|$ can be done within some scheme of unitarization (e.g. eikonal, quasieikonal, U -matrix) where pomeron rescatterings or cuts are taking into account.

However another way, the third one from the above mentioned, is possible. Here we concentrated on the dipole and tripole pomeron models. Without any details we note that these models describe the same small- $|t|$ differential cross sections with a comparable quality as the model [13] does ($\chi^2/dof \lesssim 1.05$, $dof \equiv$ degrees of freedom). The aim of the given paper is to show how the data on elastic scattering at low and middle t of protons and antiprotons on protons can be described in the dipole and tripole pomeron models.

In Sec. 2 we remind the general restrictions on hardness of pomeron singularity and form of its trajectory at small t , following from unitarity bounds on cross sections. In Sec. 3 and in Sec. 4 parametrizations of pp and $\bar{p}p$ elastic scattering amplitudes are written out in details within dipole and tripole pomeron models, correspondingly. Results of minimization for both models as well as their comparison are given in the Sec. 5.

2 General constraints

Let us remind here that the model with $\sigma_t(s) \propto \ln^2 s$ is not compatible with a linear pomeron trajectory having the intercept 1. Indeed, let assume that

$$\alpha_P(t) = 1 + \alpha'_P t$$

and the partial wave amplitude has the form

$$\varphi(j, t) = \eta(j) \frac{\beta(j, t)}{[j - 1 - \alpha'_P t]^n} \approx \frac{i\beta(1, t)}{[j - 1 - \alpha'_P t]^n}, \quad \eta(j) = \frac{1 + e^{-i\pi j}}{-\sin\pi j}. \quad (1)$$

In (s, t) -representation φ is transformed to

$$a(s, t) = \frac{1}{2\pi i} \int dj \varphi(j, t) e^{\xi(j-1)}, \quad \xi = \ln(s/s_0). \quad (2)$$

Thus, we have for pomeron contribution at large s

$$a(s, t) \approx -g(t) [\ln(-is/s_0)]^{n-1} (-is/s_0)^{\alpha'_P t}, \quad \text{where } g(t) = \beta(t)/\sin(\pi\alpha_P(t)/2). \quad (3)$$

If as usually $g(t) = g \exp(bt)$ then one can obtain

$$\sigma_t(s) \propto \ln^{n-1} s, \quad \sigma_{el}(s) \propto \frac{1}{s^2} \int_{-\infty}^0 dt |a(s, t)|^2 \propto \ln^{2n-3} s. \quad (4)$$

From the evident inequality

$$\sigma_{el}(s) \leq \sigma_t(s) \quad (5)$$

we have

$$2n - 3 \leq n - 1 \quad \Rightarrow \quad n \leq 2. \quad (6)$$

Thus it is incorrect to construct a model with $\sigma_t(s) \propto \ln^2 s$ and with a linear pomeron trajectory, by other words to use for partial amplitude Eq. (1) putting $n = 3$ (as it was done in some papers).

If $n = 1$ we have the simplest case: simple pole leading to constant total cross section and vanishing elastic cross section. However this case ($\sigma_t(s) \rightarrow const$ at $s \rightarrow \infty$) is not supported by experimental data.

If $n = 2$ we have the model of dipole pomeron ($\sigma_t(s) \propto \ln(s)$). We would like to emphasize that double pole is the most hard singularity of partial amplitude allowed by unitarity bound (5) provided its trajectory is linear at $t \approx 0$.

Thus, if one want to construct the model giving cross section that rises faster than $\ln(s)$, it is necessary to consider a more complicated case:

$$\varphi(j, t) = \eta(j) \frac{\beta(j, t)}{[j - 1 + k(-t)^{1/\mu}]^n} \approx \frac{i\beta(1, t)}{[j - 1 + k(-t)^{1/\mu}]^n}. \quad (7)$$

Making use of the same arguments as above, we obtain

$$\sigma_t(s) \propto \ln^{n-1} s, \quad \sigma_{el}(s) \propto \ln^{2n-2-\mu} s \quad \text{and} \quad \mu \geq n - 1. \quad (8)$$

However in this case amplitude $a(s, t)$ has a branch point at $t = 0$ which is forbidden by analyticity.

A more correct form of amplitude leading to t_{eff}^{-1} decreasing faster than $1/\ln s$ (it is necessary for σ_t rising faster than $\ln s$) is the following

$$\varphi(j, t) = \eta(j) \frac{\beta(j, t)}{[(j - 1)^m - kt]^n}. \quad (9)$$

¹ t_{eff} can be defined as following. If $A(s, t) \approx sf(s)F(t/t_{eff}(s))$ at $s \rightarrow \infty$ then $\sigma_{el}(s) \propto |f(s)|^2 \int_{-\infty}^0 dt |F(t/t_{eff})|^2 = t_{eff} |f(s)F(1)|^2$

Now in j -plane we have m branch points, which are collided at $t = 0$ creating the pole of order m at $j = 1$ but there is no branch point in t at $t = 0$. At the same time $t_{eff} \propto 1/\ln^m s$. From the $\sigma_{el} \propto \ln^{2mn-2-m} s \leq \sigma_t \propto \ln^{mn-1} s \leq \ln^2 s$ one can obtain

$$\begin{cases} mn \leq m + 1, \\ mn \leq 3. \end{cases} \quad (10)$$

If $\sigma_{el} \propto \sigma_t$ then $n = 1 + \frac{1}{m}$. Furthermore if $\sigma_t \propto \ln s$ then $m = 1$ and $n = 2$, it is the dipole pomeron model. In the tripole pomeron model $m = 2$ and $n = 3/2$ which lead to $\sigma_t \propto \ln^2 s$.

3 Dipole parametrizations

In this model the dominating at high energy term (double pole) is

$$\varphi_d(j, t) \propto \frac{1}{(j - 1 - \alpha'_d t)^2}. \quad (11)$$

One can say basing on the inequalities (10) that the double pole is the unitarity limit for linear ($m = 1$) pomeron trajectory. It is quite natural to add to the partial amplitude next, less singular, term (simple pole which may have trajectory with a different slope) and write dipole pomeron model in the form

$$\varphi(j, t) = \eta(j) \frac{\beta_d(t)}{(j - 1 - \alpha'_d t)^2} + \eta(j) \frac{\beta_s(t)}{j - 1 - \alpha'_s t} \quad (12)$$

which can be rewritten in (s, t) representation

$$a(s, t) = g_d \ln(-iz) (-iz)^{1+\alpha'_d t} \exp(b_d t) + g_s (-iz)^{1+\alpha'_s t} \exp(b_s t), \quad (13)$$

where variable z is proportional to cosine of scattering angle in t -channel

$$z = (t + 2(s - 2m_p^2))/z_0, \quad z_0 = 1\text{GeV}^2 \quad (14)$$

Generally form factors (or residues) may be chosen in various forms (e.g. exponential, factorized powers). However in what follows we consider for simplicity the exponential ones.

Instead of f, ω and ρ, a_2 (the last two reggeons are smaller than the first pair) let consider two effective reggeons: crossing-even, $R_+(s, t)$, and crossing-odd, $R_-(s, t)$. Contribution of them we take into account in the standard form, however with additional factor $Z_R(t)$ that changes a sign at some t ².

$$R(s, t) = \eta_R g_R Z_R(t) (-iz)^{\alpha_R(t)} \exp(b_R t), \quad (15)$$

where $\eta_R = -1/\sin(0.5\pi\alpha_+(0))$ for R_+ -reggeon and $\eta_R = i/\cos(0.5\pi\alpha_-(0))$ for R_- -reggeon. Evidently these terms are very close to f - and ω -reggeons, correspondingly. We use the same factors $Z_R(t)$ as in [14]:

$$Z_R(t) = \frac{\tanh(1 + t/t_R)}{\tanh(1)}. \quad (16)$$

²For crossing-odd term of amplitude such a factor is known a long time, it describes crossover effect, i.e. intersection of the ab and $\bar{a}b$ differential cross sections at $t \approx -0.15 \text{ GeV}^2$. Our analysis [14] showed that similar factor is visible in crossing-even reggeon term.

Our aim is to consider wide regions of s ($\sqrt{s} \geq 5$ GeV) and t ($0.1 \leq |t| \leq 6$ GeV²)³. To have a good description of the differential cross sections one need to add a few extra terms. First of all it is an odderon contribution. The existing data on total cross section and parameters $\rho = \Re a(s, 0)/\Im a(s, 0)$, as it is well known, do not show any visible odderon, but certainly it is appeared to give the difference of pp and $\bar{p}p$ differential cross sections at $\sqrt{s} = 53$ GeV and t around the dip. So we add the odderon contribution vanishing at $t = 0$

$$\begin{aligned} \mathcal{O}(s, t) = t^2 z Z_{R_-}(t) & \left\{ o_1 \ln^2(-iz) \exp(b_{o1}t) \right. \\ & \left. + o_2 \ln(-iz) \exp(b_{o2}t) + o_3 \exp(b_{o3}t) \right\} (-iz)^{1+\alpha'_o t}. \end{aligned} \quad (17)$$

Term $\propto \ln^2(s)$ in the above expression does not violate unitarity restriction $\sigma_{el}(s) \leq \sigma_t(s)$ at very large s due to factor t^2 because $\sigma_{el} \propto t_{eff}^3 \ln^4 s$, in the dipole model $t_{eff} \sim 1/\ln s$, therefore $\sigma_{el} \propto \ln s$.

At high energy and at $t = 0$ two main rescatterings terms of dipole pomeron (or cut terms) have the same form as the input amplitude: double pole plus simple pole. It means that comparing the model with experimental data we can not distinguish unambiguously between input terms and cuts. So at $t = 0$ one can use only an input amplitude. At $t \neq 0$ situation is more complicated because the slopes of trajectories in cut terms differ from the input one. These terms can be important at large $|t|$ but they in fact are already taken into account at $t = 0$.

Having in mind the above arguments and in order do not destroy a good description of the data at $t = 0$ we write pomeron, pomeron-pomeron and pomeron-reggeons cuts vanishing at $t = 0$. It is not true rescatterings but they mimic them efficiently. Thus we write:

pomeron contribution

$$P(s, t) = -g_P (-iz)^{1+\alpha'_P t} [\exp(b_{P1}t) - \exp(b_{P2}t)], \quad (18)$$

pomeron-pomeron cut

$$C_P(s, t) = -\frac{t}{\ln(-iz)} g_{PP} (-iz)^{1+\alpha'_P t/2} \exp(b_{PP}t), \quad (19)$$

pomeron-even reggeon cut

$$C_{R_+}(s, t) = -\frac{t Z_{R_+}(t)}{\ln(-iz)} \eta_{R_+} g_{P+} Z_{R_+}(t) (-iz)^{\alpha_+(0)+\alpha'_{P+} t} \exp(b_{P+}t), \quad (20)$$

where

$$\alpha'_{P+} = \frac{\alpha'_P \alpha'_{R_+}}{\alpha'_P + \alpha'_{R_+}}, \quad (21)$$

pomeron-odd reggeon cut

$$C_{R_-}(s, t) = -i \frac{t Z_{R_-}(t)}{\ln(-iz)} \eta_{R_-} g_{P-} Z_{R_-}(t) (-iz)^{\alpha_-(0)+\alpha'_{P-} t} \exp(b_{P-}t), \quad (22)$$

$$\alpha'_{P-} = \frac{\alpha'_P \alpha'_{R_-}}{\alpha'_P + \alpha'_{R_-}}. \quad (23)$$

Writing them with arbitrary constants b we keep a some phenomenological freedom in a t -dependence.

³A more complicated than exponential form for residues should be considered for larger $|t|$.

4 Tripole pomeron model

As it follows from Eq.(10) for the dominating contribution in a tripole pomeron model with $\sigma_t(s) \propto \ln^2(s)$, i.e. $n = 2$, $m = 3/2$, we should write

$$\varphi_1(j, t) = \eta(j) \frac{\beta_1(j, t)}{[(j-1)^2 - kt]^{3/2}}. \quad (24)$$

It seems to be natural to write the subleading terms as the following

$$\varphi_2(j, t) = \eta(j) \frac{\beta_2(j, t)}{[(j-1)^2 - kt]}, \quad (25)$$

$$\varphi_3(j, t) = \eta(j) \frac{\beta_3(j, t)}{[(j-1)^2 - kt]^{1/2}}. \quad (26)$$

Thus amplitude is written as

$$\varphi(j, t) = \varphi_1(j, t) + \varphi_2(j, t) + \varphi_3(j, t) + R(j, t) \quad (27)$$

where $R(j, t)$ is a contribution of other reggeons and possible cuts (which are important at low energies and probably at large $|t|$).

From the tabular integrals

$$\int_0^\infty dx x^{\alpha-1} e^{-\omega x} J_\nu(\omega_0) = I_\nu^\alpha \quad (28)$$

where

$$I_\nu^{\nu+1} = \frac{(2\omega_0)^\nu}{\sqrt{\pi}} \frac{\Gamma(\nu + 1/2)}{(\omega^2 + \omega_0^2)^{\nu+1/2}},$$

$$I_\nu^{\nu+2} = 2\omega \frac{(2\omega_0)^\nu}{\sqrt{\pi}} \frac{\Gamma(\nu + 3/2)}{(\omega^2 + \omega_0^2)^{\nu+3/2}},$$

one can find

$$\frac{1}{(\omega^2 + \omega_0^2)^{3/2}} = \frac{1}{2\omega_0} \int_0^\infty dx x e^{-x\omega} J_1(\omega_0 x), \quad (29)$$

$$\frac{1}{\omega^2 + \omega_0^2} = \frac{1}{\omega_0} \int_0^\infty dx e^{-x\omega} \sin(x\omega_0) \quad (30)$$

and

$$\frac{1}{(\omega^2 + \omega_0^2)^{1/2}} = \int_0^\infty dx e^{-x\omega} J_0(\omega_0 x). \quad (31)$$

Thus tripole amplitude with the subleading terms can be written as following

$$a_{tr}(s, t) = iz \left\{ g_{+1} \exp(b_{+1}t) \ln(-iz) \frac{2J_1(\xi_+ \tau_+)}{\tau_+} + g_{+2} \frac{\sin(\xi_+ \tau_+)}{\tau_+} \exp(b_{+2}t) + g_{+3} J_0(\xi_+ \tau_+) \exp(b_{+3}t) \right\} \quad (32)$$

where $\xi_+ = \ln(-iz) + \lambda_+$, z is defined by Exp.(14), and $\tau_+ = r_+ \sqrt{-t/t_0}$, $t_0 = 1 \text{ GeV}^2$, r_+ is a constant.

Similar expression one can write for odderon contribution but multiplying it by factors t and $Z_{R_-}(t)$

$$\mathcal{O}(s, t) = ztZ_{R_-}(t) \left\{ g_{-1} \ln(-iz) \frac{2J_1(\xi_- \tau_-)}{\tau_-} \exp(b_{-1}t) + g_{-2} \frac{\sin(\xi_- \tau_-)}{\tau_-} \exp(b_{-2}t) + g_{-3} J_0(\xi_- \tau_-) \exp(b_{-3}t) \right\}. \quad (33)$$

where $\xi_- = \ln(-iz) + \lambda_-$ and $\tau_- = r_- \sqrt{-t/t_0}$.

Again, to describe the data at low energies we add the ‘‘soft’’ pomeron

$$P(s, t) = -g_P(-iz)^{1+\alpha'_P t} \exp(b_P t), \quad (34)$$

reggeon and cut contributions which are written in the same form as in dipole pomeron model (Eqs.19,20,22).

AGLN-model. Let us to give a few comment about another version of tripole pomeron model presented in the papers [6, 7].

1. If $\xi = \ln(-is/s_0)$, $s_0 = 1 \text{ GeV}^2$, then the first pomeron term in [6, 7] is the same as in (32) while for the second and third terms authors write

$$g_2(t) \xi J_0(\xi \tau)$$

which corresponds to the partial amplitude

$$\varphi(j, t) = \eta(j) g_2(t) \frac{2(j-1)}{[(j-1)^2 - kt]^{3/2}},$$

and

$$g_3(t) [J_0(\xi \tau_+) - \xi_0 \tau_+ J_1(\xi \tau_+)]$$

corresponding to

$$\varphi(j, t) = \eta(j) g_2(t) \frac{(j-1)^2 + kt}{[(j-1)^2 - kt]^{3/2}}.$$

2. Another form of odderon terms is used also. The maximal odderon contribution

$$\mathcal{O}_m(s, t) = g_{-1} \ln^2(-iz) \frac{\sin(\xi \tau_-)}{\tau_-} \exp(b_{-1}t) + g_{-2} \ln(-iz) \cos(\xi \tau_-) \exp(b_{-2}t) + g_{-3} \exp(b_{-3}t) \quad (35)$$

as well as a simple pole odderon and odderon-pomeron cut are taken into account.

3. Omitting many details of the model we note that because of the chosen form of signature factors it has pole at $t = -1/\alpha' = -4 \text{ GeV}^2$. This defect of the model restricts the applicability region. Similar poles even at less values of $|t|$ AGLN-amplitude has in the reggeon terms. Thus the model must be modified to describe a more wide than was considered in [7] region of t , namely $|t| \leq 2.6 \text{ GeV}^2$.

4. In our opinion this model leads to unreasonable intercept of the crossing-odd reggeon, $\alpha_-(0) = 0.34$. Such intercept strongly contradicts to the values known from spectroscopy data on meson resonances although one can expect it to be closed to intercept of ω -trajectory, $\alpha_\omega(0) \approx 0.43 - 0.46$ [11].

Nevertheless in the Section 5 in order to compare AGLN model with our dipole and tripole models we show the curves obtained at this model for differential cross sections at available and LHC energies.

5 Comparison with experimental data

5.1 Total cross sections

Describing the pp and $\bar{p}p$ data we have in mind a further extension of the models for elastic $\pi^\pm p$ and $K^\pm p$ scattering, there are more or less precise data on these processes. One circumstance is important enough to be taken into account. Fit to σ_t and ρ in case of pp and $\bar{p}p$ leads to the set of parameters which is quite strongly differed of those obtained from the fit to all proton(antiproton) π - and K -meson data.

For the above reason we take the following fitting procedure. At the first stage we determine all parameters that control amplitudes at $t = 0$. We use the standard data set for the $\pi^\pm p$ and $K^\pm p$ total cross sections and the ratios ρ (at $5 \text{ GeV} \leq \sqrt{s} < 2000 \text{ GeV}$) [15] to find intercepts of C_\pm -reggeons and couplings of the reggeon and pomeron exchanges. In the considered region there are 542 experimental points (see Table 1).

An extension of the above written $pp \rightarrow pp$ and $\bar{p}p \rightarrow \bar{p}p$ dipole and tripole amplitudes for $\pi^\pm p$ and $K^\pm p$ elastic scattering is quite evident. Only couplings are different in these amplitudes at $t = 0$, and odderon does not contribute to πp and $K p$ amplitudes. In the simplest unitarization schemes (eikonal, U -matrix) all cross sections at asymptotically high energies have an universal behaviour, $\sigma_t(s) \rightarrow \sigma_0 \log^2(s_{ap}/s_0)$, where σ_0 does not depend on the sort of initial particles. Fit to the available data does not contradict to this conclusion. So in the tripole model we put equal couplings for the main pomeron terms in all amplitudes $g_{+1}^p = g_{+1}^\pi = g_{+1}^K$. Beside this to avoid uncertainty at $t = 0$ (constant contributions to total cross sections are coming additively from the third term of Eq.(32) and from ‘‘soft’’ pomeron, Eq.(34)) we replace couplings g_{+3} for $g_{+3} - g_P$ in Eq.(32). As a result, only g_{+3} give energy independent contribution to the total cross sections.

The following normalization of $ab \rightarrow ab$ amplitude is used

$$\sigma_t = \frac{1}{s_{ab}} \Im m A(s, 0), \quad \frac{d\sigma}{dt} = \frac{1}{16\pi s_{ab}^2} |A(s, t)|^2 \quad (36)$$

where

$$s_{ab} = \sqrt{(s - m_a^2 - m_b^2)^2 - 4m_a^2 m_b^2} = 2p_a^{lab} \sqrt{s}$$

and p_a^{lab} is the momentum of hadron a in laboratory system of b .

The details of the fit at $t = 0$ are presented in the Tables 1 and 2.

5.2 Differential cross sections

At the second stage of the fitting procedure we fix all intercepts and couplings obtained at the first stage. Other parameters are determined from the fit to data on $d\sigma/dt$ in region

$$0.1 \text{ GeV}^2 \leq |t| \leq 6 \text{ GeV}^2, \quad \sqrt{s} \geq 5 \text{ GeV}. \quad (37)$$

Many measurements of the differential elastic cross sections was done in last 40 years. Fortunately, most of these measurements have been communicated to the Durham Data Base [16], so that one does not need to re-encode all the data. However, there are 80 papers, with different conventions, and various units. The complete list of the references is given in the paper [14]. We have uniformly formatted them, found and corrected some errors in the sets, gave detailed description of the full set that contains about 10000 points. Analyzing

Table 1: Quality of the fit to σ_t and ρ

		χ_{tot}^2/N_p	
quantity	number of data	Dipole model	Tripole model
σ_t^{pp}	104	0.88260E+00	0.87055E+00
$\sigma_t^{\bar{p}p}$	59	0.95280E+00	0.96273E+00
$\sigma_t^{\pi^+p}$	50	0.66216E+00	0.66792E+00
$\sigma_t^{\pi^-p}$	95	0.10023E+01	0.99864E+00
$\sigma_t^{K^+p}$	40	0.72357E+00	0.72104E+00
$\sigma_t^{K^-p}$	63	0.61392E+00	0.60883E+00
ρ^{pp}	64	0.16612E+01	0.16965E+01
$\rho^{\bar{p}p}$	11	0.40392E+00	0.40675E+00
ρ^{π^+p}	8	0.15107E+01	0.15036E+01
ρ^{π^-p}	30	0.12560E+01	0.12122E+01
ρ^{K^+p}	10	0.10869E+01	0.10016E+01
ρ^{K^-p}	8	0.12185E+01	0.11611E+01
Total		χ_{tot}^2/dof	
	542	0.99450E+00	0.99345E+00

each subset of these data in [14] we payed attention mainly to the data at small t . Some of subsets which are in strong disagreement with the rest of the dataset were excluded from the fit. A similar work was performed for the data at $|t| > 0.7 \text{ GeV}^2$. Again we found some mistakes in the data base as well as have excluded a few subset ⁴ from the final dataset which was used for fitting. Thus the considered models were fitted to 2532 points on $d\sigma/dt$ in region (37). The results are given in the Table 3 for a quality of fit and in the Table 4 for the fitted parameters.

In the figures 1 - 5 we show experimental data at some selected energies and theoretical curves obtained in three models: AGLN [7], Dipole and Tripole. Regarding the AGLN-model, we would like to emphasize that presented curves were calculated at the parameters given in [7]. However, in contrast to Dipole and Tripole models it was fitted to differential cross sections at $\sqrt{s} > 9.7 \text{ GeV}$ and $|t| < 2.6 \text{ GeV}^2$ as well as not to complete dataset. Therefore a disagreement between curves and data at lowest energy in the given model is not surprising. One can see that AGLN-model well works at high energies.

6 Conclusion

In this paper we compare three unitarized models of elastic scattering amplitude fitting the Dipole and Tripole models to all existing data. We emphasize that the amplitude leading to $\sigma_t \propto \ln^2 s$ should be parameterized with a special care because of the restrictions on a form and properties of the main partial wave singularity that follow from unitarity and analyticity.

As one can see from the Figures and Tables the considered models well describe the data (AGLN model does not describe low energy data but it was fitted to the data only at

⁴We excluded the subsets [17] at $\sqrt{s} = 9.235 \text{ GeV}$, [18] at $\sqrt{s} = 19.47, 27.43 \text{ GeV}$ from pp data and [20] at $\sqrt{s} = 7.875 \text{ GeV}$, [21] at $\sqrt{s} = 9.778 \text{ GeV}$ from $\bar{p}p$ data because they strongly contradict to the rest of data.

Table 2: Intercepts and couplings (GeV^{-2}) in the Dipole and Tripole models from the fit to σ_t and ρ

Dipole model			Tripole model		
param.	value	error	param.	value	error
$\alpha_{R+}(0)$	0.80846E+00	0.36035E-02	$\alpha_{R+}(0)$	0.71947E+00	0.18496E-02
$\alpha_{R-}(0)$	0.46505E+00	0.91416E-02	$\alpha_{R-}(0)$	0.46356E+00	0.73746E-02
g_d^p	0.89435E+01	0.19499E+00	g_{+1}^p	0.15330E+02	0.31619E+00
g_s^p	-0.52159E+02	0.30078E+01	g_{+2}^p	0.19153E+01	0.38589E-01
g_{R+}^p	0.15857E+03	0.30846E+01	g_{+3}^p	0.20672E+00	0.26747E-02
g_{R-}^p	0.58961E+02	0.28775E+01	g_{R+}^p	0.96906E+02	0.84678E+00
g_d^π	0.70477E+01	0.22719E+00	g_{R-}^p	0.59294E+02	0.23228E+01
g_s^π	-0.45720E+02	0.29022E+01	g_{+1}^π	0.69901E+01	0.18396E+00
g_{R+}^π	0.10691E+03	0.33590E+01	g_{+2}^π	0.10106E+01	0.27123E-01
g_{R-}^π	0.10710E+02	0.52507E+00	g_{R+}^π	0.56296E+02	0.45360E+00
g_d^K	0.54351E+01	0.29205E+00	g_{R-}^π	0.10784E+02	0.43687E+00
g_s^K	-0.29703E+02	0.33234E+01	g_{+1}^K	0.12186E+02	0.22424E+00
g_{R+}^K	0.70785E+02	0.43792E+01	g_{+2}^K	0.14683E+00	0.30439E-01
g_{R-}^K	0.23674E+02	0.11159E+01	g_{R+}^K	0.28730E+02	0.51047E+00
			g_{R-}^K	0.23831E+02	0.91697E+00

Table 3: Quality of the fit to $d\sigma/dt$

	Number of points, N_p	χ_{tot}^2/N_p	
		Dipole model	Tripole model
$d\sigma^{pp}/dt$	1857	0.15122E+01	0.18153E+01
$d\sigma^{pp}/dt$	675	0.14183E+01	0.16697E+01

$\sqrt{s} > 9.7$ GeV, we did not refit it). However the obtained χ^2 (Table 3) testifies that the Dipole pomeron model is in a slightly better agreement with data.

The most interesting and important fact for further choice of the best model is shown on Fig. 5. Predictions of the compared models for pp cross section at LHC energy are strongly different at $|t|$ around 0.3 - 0.5 GeV^2 . Certainly the future TOTEM measurement will allow to distinguish between three considered models.

I would like to thank Prof. B. Nicolescu and Dr. J.R. Cudell for many useful discussions.

The work was supported partially by the Ukrainian Fund of Fundamental Researches.

References

- [1] A. Donnachie and P.V. Landshoff, Phys. Lett. **B296** (1992) 227; P.V. Landshoff, arXiv:hep-ph/0509240; Nucl. Phys. Proc. Suppl. **A99** (2001) 311, [arXiv:hep-ph/0010315] and references therein.
- [2] M. Giffon, P. Desgrolard and E. Predazzi, Z. Phys. **C63** (1994) 241.

- [3] Discussion of an eikonal approximation in the Regge theory as well as references to the original papers on this subject can be found in P.D.B. Collins, *An introduction to Regge theory & high energy physics*, Cambridge University press (Cambridge) 1977;
See also: K.A. Ter-Martirosyan, *Sov. ZhETF Pisma* **15** (1972) 519;
V.A. Petrov and A.V. Prokudin, *Eur. Phys. J.* **C23** (2002) 135;
C. Bourrely, J. Soffer and T.T. Wu, *Eur. Phys. J. C* **28** (2003) 97 [arXiv:hep-ph/0210264];
P.A.S. Carvalho, A.F. Martini and M.J. Menon, *Eur. Phys. J.* **C39** (2005) 359 [arXiv:hep-ph/0312243].
- [4] S.M. Troshin and N.E. Tyurin, *Phys. Part. Nucl.* **35** (2004) 555; *Fiz. Elem. Chast. Atom. Yadra* **35** (2004) 1029; [arXiv:hep-ph/0308027] and references therein;
L.L. Jenkovszky, B.V. Struminsky and A.N. Wall, *Sov. Journ. Part. Nucl.* **19** (1988) 180.
- [5] L. Lukaszuk and B. Nicolescu, *Nuovo Cimento Letters* **8** 405 1973;
P. Gauron, E. Leader and B. Nicolescu, *Nuclear Physics* **B299** 640 (1988).
- [6] P. Gauron, E. Leader and B. Nicolescu, *Phys. Lett.* **B238** (1990) 406.
- [7] R. Avila, P. Gauron and B. Nicolescu, *Eur. Phys. J.* **C49** (2007) 581-592 [arXiv:hep-ph/0607089].
- [8] L.L. Jenkovszky, E.S. Martynov and B.V. Struminsky, *Phys. Lett.* **B249** (1990) 535.
- [9] P. Desgrolard, M. Giffon, E. Martynov and E. Predazzi, *Eur. Phys. J.* **C18** (2000) 359.
- [10] J.R. Cudell *et al.*, *Phys. Rev.* **D65**, 074024 (2002) [arXiv:hep-ph/0107219]; J.R. Cudell *et al.*, *Phys. Rev. Lett.* **89** (2002) 201801; [arXiv:hep-ph/0206172].
- [11] P. Desgrolard, M. Giffon, E. Martynov and E. Predazzi, *Eur. Phys. J.* **C18** (2001) 555 [arXiv:hep-ph/0006244].
- [12] J.R. Cudell, E. Martynov and O. Selyugin, *Eur. Phys. J.* **C33** (2004) s533; [arXiv:hep-ph/0311019].
- [13] J.R. Cudell, A. Lengyel and E. Martynov, *Phys. Rev.* **D73** (2006) 034008 [arXiv:hep-ph/0511073].
- [14] J.R. Cudell, E. Martynov, O. Selyugin and A. Lengyel, *Phys. Lett.* **B587** (2004) 78 [arXiv:hep-ph/0310198].
- [15] Review of Particle Physics, S. Eidelman *et al.*, *Phys. Lett.* **B592** (2004) 1. Encoded data files are available at <http://pdg.lbl.gov/2005/hadronic-xsections/hadron.html>.
- [16] Durham Database Group (UK), M.R. Whalley *et al.*, <http://durpdg.dur.ac.uk/hepdata/reac.html>.
- [17] C. Bruneton *et al.*, *Nucl. Phys.* **B 124** (1977) 391.
- [18] S. Conetti *et al.*, *Phys. Rev. Lett.* **41** (1978) 924.

- [19] J.C.M. Armitage *et al.*, Nucl. Phys. **B132** (1978) 365.
- [20] M.Y. Bogolyubsky *et al.*, Yad. Fiz. **41** (1985) 1210 [Sov. J. Nucl. Phys. **41** (1985) 773].
- [21] C.W. Akerlof *et al.*, Phys. Rev. **D14** (1976) 2864.

Table 4: Parameters of the models, from the fit to $d\sigma/dt$ (parameters r_{\pm}, λ_{\pm} are dimensionless, $t_{R\pm}$ are given in GeV^2 , the rest parameters are given in GeV^{-2}).

Dipole model			Tripole model		
param.	value	error	param.	value	error
α'_d	0.30631E+00	0.16923E-02	r_+	0.25417E+00	33181E-02
α'_s	0.28069E+00	0.19026E-03	λ_+	0.11575E+01	14824E+00
b_d	0.38675E+01	0.22767E-01	b_{+1}	0.34583E+01	37982E-01
b_s	0.55679E+00	0.14694E-02	b_{+2}	0.19091E+01	30598E-01
α'_{R+}	0.82000E+00	fixed	b_{+3}	0.45970E+00	29750E-02
b_{R+}	0.29226E+01	0.30019E-01	α'_{R+}	0.82000E+00	fixed
t_{R+}	0.48852E+00	0.26683E-02	b_{R+}	0.10668E+01	30350E-01
α'_{R-}	0.91000E+00	fixed	t_{R+}	0.54237E+00	13817E-01
b_{R-}	0.15201E+01	0.68671E-01	α'_{R-}	0.91000E+00	fixed
t_{R-}	0.14497E+00	0.24811E-02	b_{R-}	0.61435E-01	20044E-01
o_1	0.30738E+00	0.31368E-02	t_{R-}	0.15755E+00	26068E-02
o_2	-0.63119E+01	0.55282E-01	r_-	0.78807E-01	60563E-02
o_3	0.13456E+00	0.21551E-02	λ_-	0.16281E+02	19020E+01
α'_o	0.21810E-01	0.70324E-03	o_1	-0.56075E-01	51702E-02
b_{o1}	0.39317E+01	0.81697E-02	o_2	0.17372E+01	17893E+00
b_{o2}	0.45007E+01	0.76861E-02	o_3	-0.61193E+02	363298E+01
b_{o3}	0.12947E+01	0.76773E-02	b_{o1}	0.12038E+01	26425E-01
g_P	0.58961E+02	0.98576E-01	b_{o2}	0.15152E+01	31722E-01
α'_P	0.30696E+00	0.20475E-03	b_{o3}	0.26331E+01	78349E-01
b_{P1}	0.54894E+00	0.15036E-02	g_P	0.16042E+02	13856E-01
b_{P2}	0.59365E+01	0.34863E-01	α'_P	0.36060E+00	76335E-02
g_{PP}	-0.39324E+02	0.36883E+00	b_P	0.14662E+01	29152E-01
b_{PP}	0.11828E+01	0.44025E-02	g_{PP}	0.91195E+01	84044E+00
g_{P+}	-0.22656E+03	0.27529E+01	b_{PP}	0.44977E+00	46404E-01
b_{P+}	0.17522E+01	0.98459E-02	g_{P+}	0.11772E+02	57753E+00
g_{P-}	-0.15255E+02	0.28213E+00	b_{P+}	0.81585E-01	28185E-01
b_{P-}	0.24068E-01	0.61336E-02	g_{P-}	0.81908E+01	88408E+00
			b_{P-}	-0.79115E-01	45833E-01

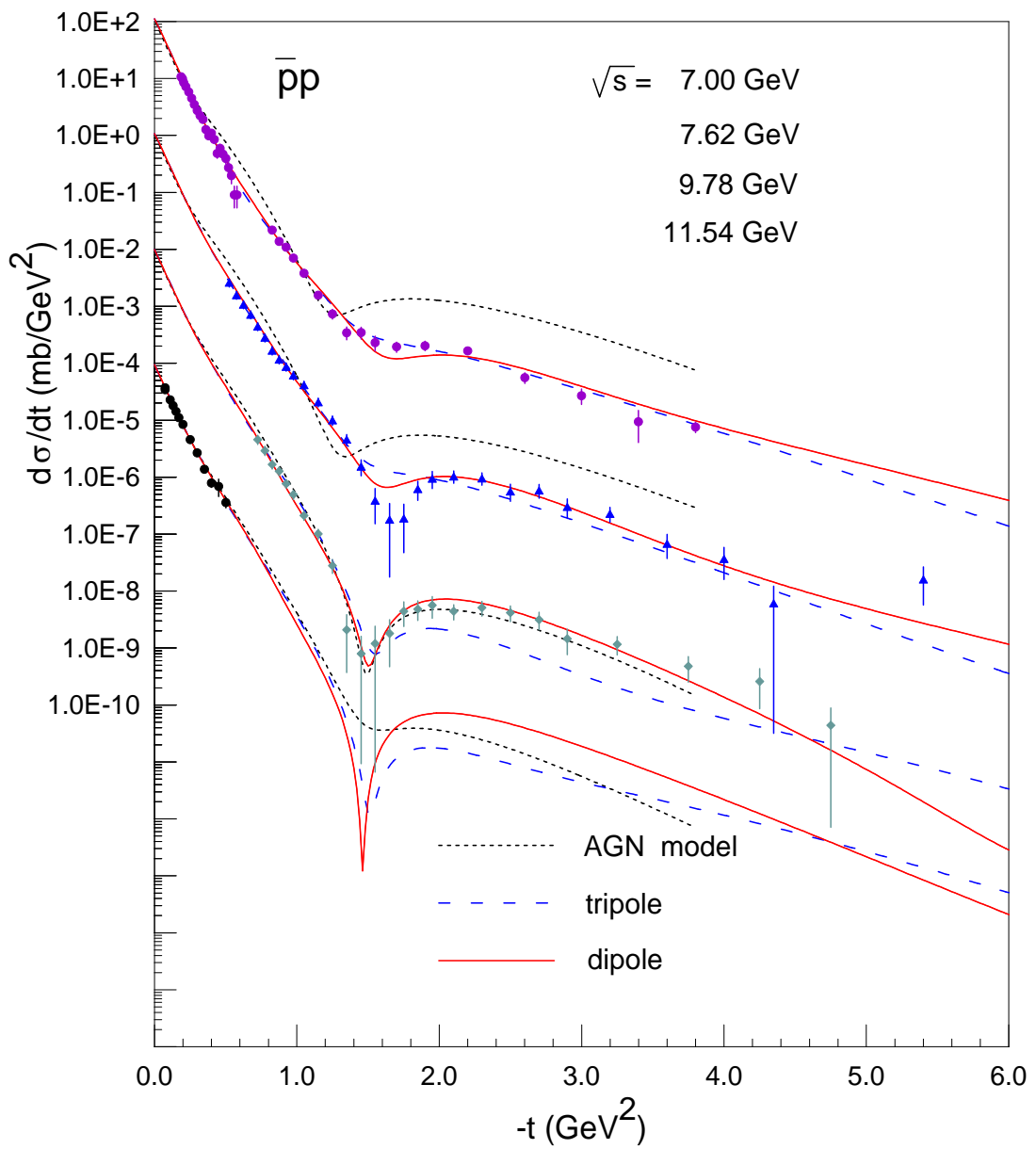


Figure 1: $\bar{p}p$ at low energies

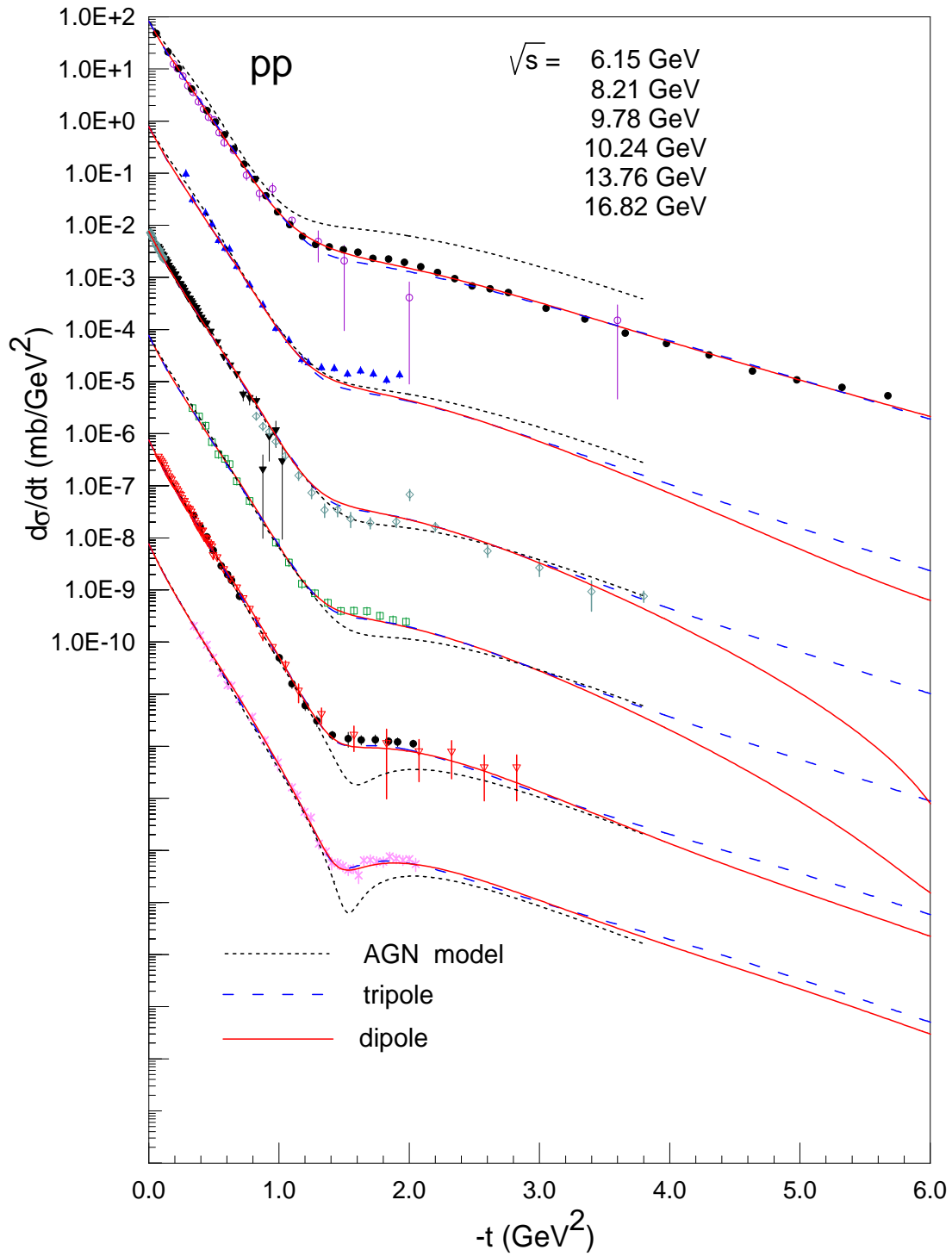


Figure 2: pp at low energies

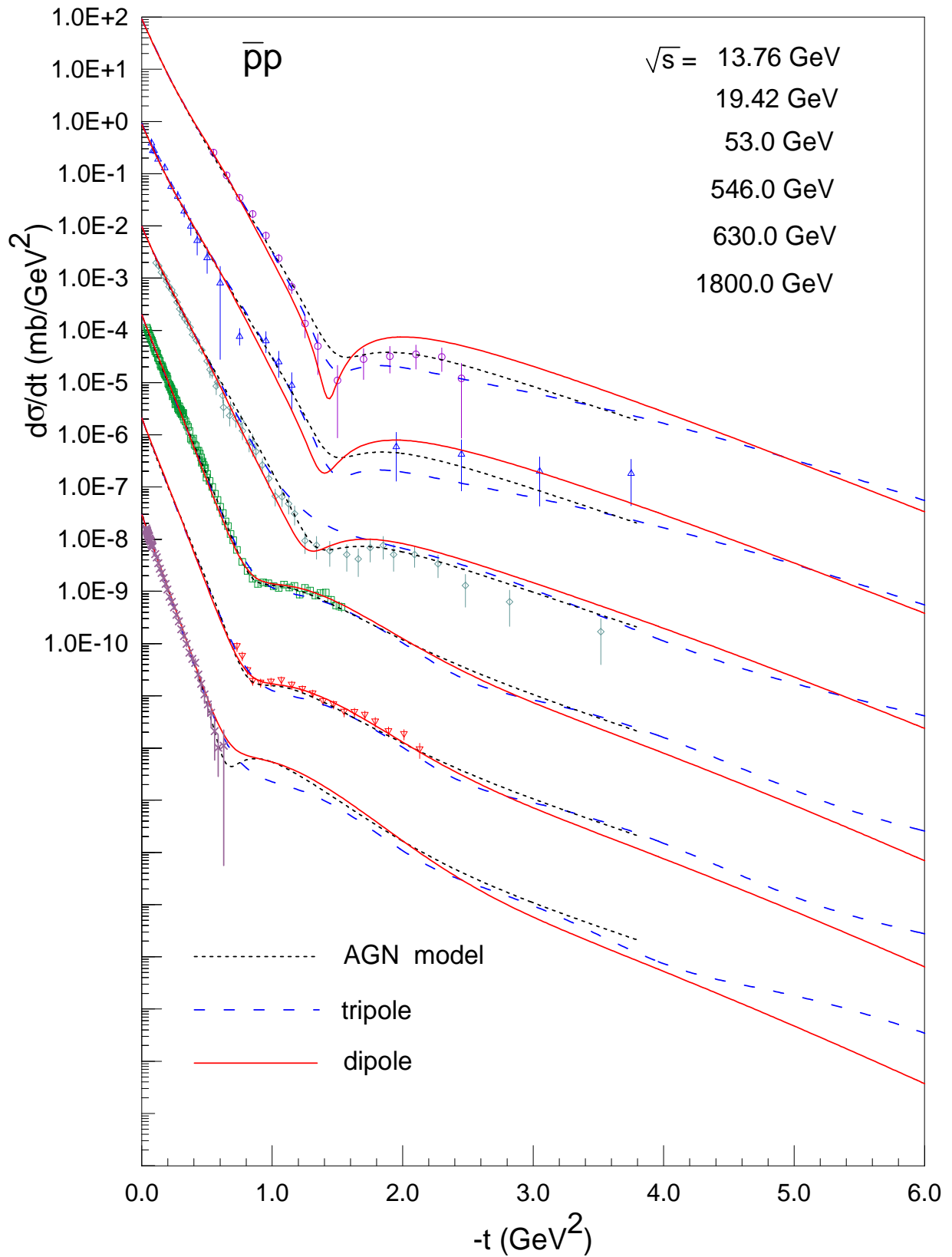


Figure 3: $\bar{p}p$ at high energies

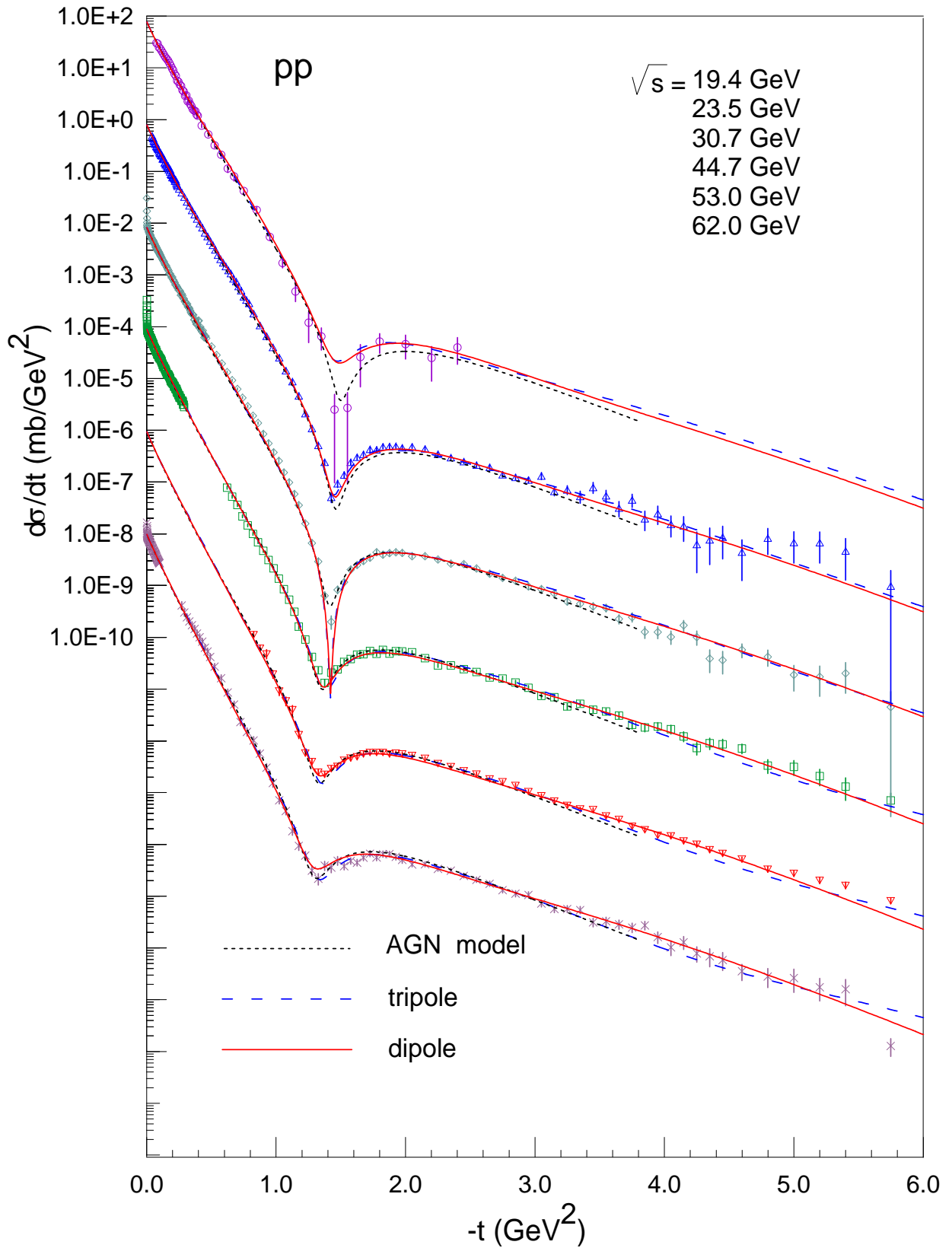


Figure 4: pp at high energies

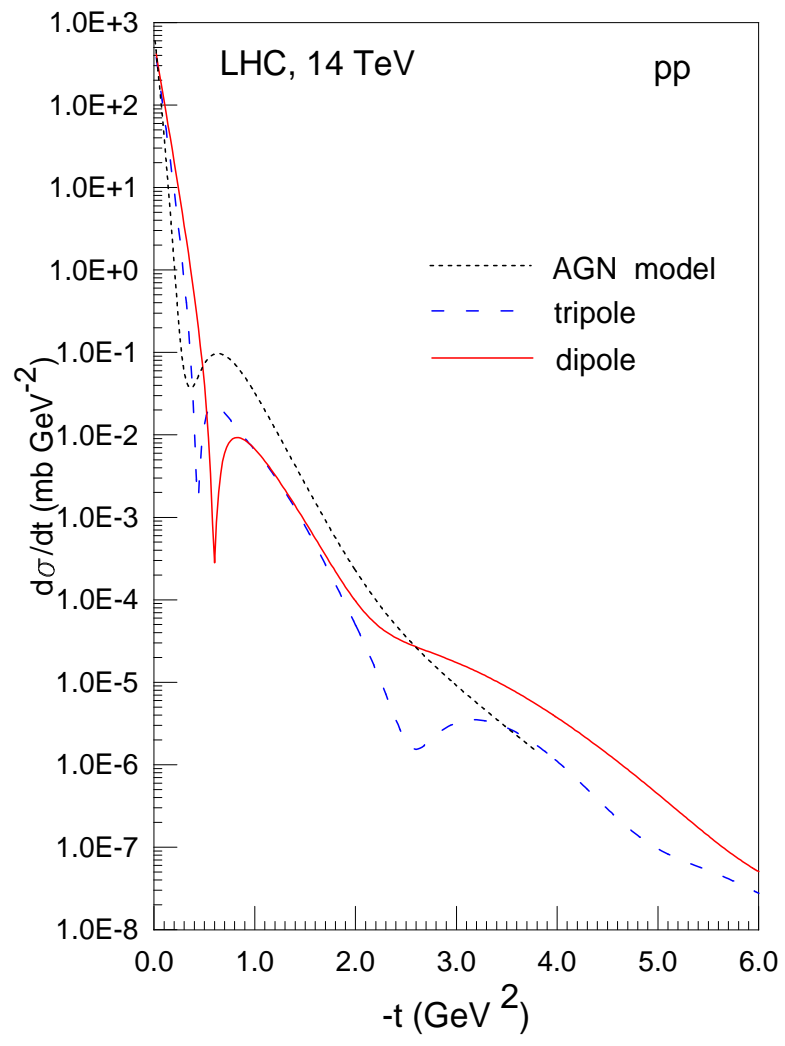


Figure 5: Predictions for LHC energy